

# CALIBRATION OF HEFT HARD X-RAY OPTICS

Jason E. Koglin<sup>1</sup>, Wayne H. Baumgartner<sup>2</sup>, C.M. Hubert Chen<sup>2</sup>, James C. Chonko<sup>1</sup>, Finn E. Christensen<sup>3</sup>,  
William W. Craig<sup>4</sup>, Todd R. Decker<sup>4</sup>, Charles J. Hailey<sup>1</sup>, Fiona A. Harrison<sup>2</sup>,  
Carsten P. Jensen<sup>3</sup>, Kristin K. Madsen<sup>3</sup>, Michael J. Pivovarov<sup>4</sup>, and Gordon Tajiri<sup>1</sup>

<sup>1</sup>Columbia Astrophysics Laboratory, 550 W. 120<sup>th</sup> St, New York, NY

<sup>2</sup>California Institute of Technology, MC 220-47, Pasadena, CA

<sup>3</sup>Danish National Space Center, 30 Juliane Maries Vej, Copenhagen, Denmark

<sup>4</sup>Lawrence Livermore National Laboratory, Mail Stop L-043, Livermore, CA

## ABSTRACT

Three hard X-ray telescopes (20-70 keV) have been produced for the *High Energy Focusing Telescope (HEFT)*, a balloon-born mission. Each focusing, Wolter-I (conic approximation) optic was calibrated *in-situ* using low-force surface metrology as they were being assembled and at the Danish National Space Center (DNSC) using a high-resolution 8 keV X-ray source after assembly. The first optic was also calibrated using 18-68 keV X-rays at the European Synchrotron Radiation Facility (ESRF). We have also fully illuminated a prototype optic using a UV source and compared the result with the above techniques. During instrument integration, a 25 keV X-ray source at a distance of 72 m was used to align the optics and confirm the expected effective area and imaging performance. The successful development of *HEFT* has led to *NuSTAR*, a Small Explorer (SMEX) satellite mission. We discuss these pre-flight calibration methods used in the *HEFT* program.

## 1. INTRODUCTION

A new generation of hard X-ray instruments is required to open the hard X-ray frontier and answer fundamental questions about our Universe:

- How are black holes distributed through the cosmos, and how do they influence the formation of galaxies like our own?
- How were the elements that compose our bodies and the Earth forged in the explosions of massive stars?
- What powers the most extreme active galaxies?

We have developed thermally-formed glass substrates and a unique mounting technique to build the high performance, lightweight telescopes with large effective area to enable new discovery in the 6-80 keV energy band. Our approach is currently being flight demonstrated through the *High Energy Focusing Telescope (HEFT)*, a balloon born mission.

Based on the success of *HEFT*, this approach will be used for the *Nuclear Spectroscopic Telescope Array (NuSTAR)*, a small explorer class satellite. The *NuSTAR* mission will be the first satellite instrument to employ focusing optics in the 6 to 80 keV hard X-ray band. These optics, together with pixelized solid state detectors developed by Caltech, will make *NuSTAR* 1000 times more sensitive than previous experiments.

In this paper we summarize the optics production process and describe several pre-flight calibration methods used in the *HEFT* program. Much of this discussion is based on previous reports by Koglin et al. 2003-2004. We also describe the pre-flight alignment process for *HEFT*, give highlights from the 2005 flight and look to the future with *NuSTAR*.

## 2. OPTICS PRODUCTION

A major accomplishment of the *HEFT* program has been the successful development of thermally-formed glass optics with performance exceeding the *HEFT* requirements. We begin with thin glass, originally developed for flat panel displays, that is smooth and flat on all relevant length scales. Our approach is to thermally form these micro-sheets using standard quartz mandrels and commercially available ovens. We begin by placing a glass micro-sheet on top of a concave mandrel inside of the oven. As the oven is heated to the appropriate forming temperature, the glass begins to form into the mandrel under the influence of gravity. Just before the glass touches the mandrel surface, the forming process is terminated by lowering the oven temperature. In this way, near net shaped optic substrates are produced without perturbing the excellent initial X-ray properties of the glass micro-sheet, even without the aid of highly polished and very expensive mandrels.

The shells are characterized immediately after they are formed for quality control of the slumping process. An optical laser scanning apparatus designed and built at Columbia's Nevis Laboratory, is used to characterize free standing cylindrical substrates. From axial scan measurements at multiple azimuth positions, the

cylindrical surface can be reconstructed using software to remove shell alignment errors. While the initial slumping parameters are roughly determined from the raw glass properties, the slumping parameters for each oven must be tuned for each new production setup (e.g., new forming mandrel radius or different glass type – AF45 or D263). This initial tuning generally takes several days, but after that, the ovens settings are normally quite stable and subsequent substrates are produced with consistent angular performance. In this way, it is only necessary to perform laser metrology periodically for quality assurance, and only small fine tuning adjustments are required over weeks of mass production slumping with the same setup.

After initial oven tuning, approximately 95% of the slumped shells were accepted for mounting for *HEFT*. Upon acceptance, the original 20 cm x ~120 degree pieces must be cut to the appropriate size – 10 cm x ~70 degrees (i.e., a quint section) – using a scribe and break technique with better than 90% yield. The pieces are then packed and shipped to the Danish National Space Center (DNSC), where the substrates are coated with depth-graded W/Si multilayers to providing good energy response extending to 70 keV (Jensen et al. 2003, Madsen et al. 2004).

Our unique mounting process involves constraining these coated mirror shells to precisely machined graphite spacers that run along the optical axis. In this process, the nominally cylindrical glass segments are forced to a conical form, and in the process, radial mismatches and some small twists in the glass are removed. In order to achieve large effective area, concentric layers of glass are stacked on top of each other starting with a titanium mandrel. Graphite spacers are first epoxied to the mandrel and then precisely machined to the correct radius and angle. Next, a layer of glass and second layer of spacers are epoxied to the first set of spacers. These spacers are then machined to the appropriate radius and angle. This process is repeated until the requisite number of layers is assembled. A key point of this process is that each layer of spacers is machined with respect to the optic axis and not the last layer of glass. In this way, there is never any stack-up error during the telescope fabrication.

Production of the first *HEFT* telescope HF1 began in May 2002 and was completed nine months later. Assembly of HF1 began using three spacers per quint section for the first 22 layers. At this point, a switch to five spacers per quint section was made. In order to make this change, an intermediate mandrel (which effectively replaced two layers) was added for structural support from which to build the subsequent 48 layers (70 layers total). The second *HEFT* flight module HF2, which was begun immediately after HF1 was completed, was assembled in a similar fashion

over the next six months. For the third *HEFT* optic module, HF3, the innermost 12 layers were omitted and the entire optic (60 layers total) was built using five spacers over the course of the next five months. Both HF2 and HF3 were assembled at an average rate of ~3.5 layers per week. These three *HEFT* optic modules are pictured in Figure 1.

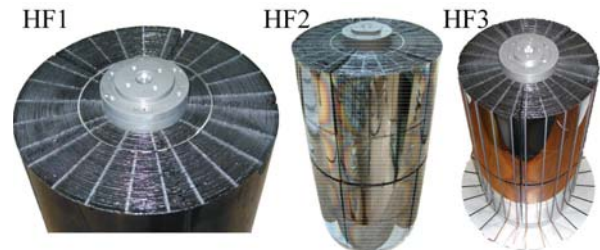


**Figure 1:** Three *HEFT* flight optics.

### 3. ANGULAR RESOLUTION

High-resolution X-ray measurements at 8.048 keV were performed on each optic at the DNSC X-ray calibration facility. A triple-axis diffractometer configuration utilized high-resolution, perfect channel-cut monochromator and analyzer crystals – both Si(220) – in a non-dispersive configuration. The optic was first aligned optically so that it rotates about its axis with no visible wobble (less than ~20”) in precisely aligned pinholes at each end of the optic module that define the optical axis. A photograph of the HF1 optic mounted for X-ray calibration is shown in Figure 2. The X-ray beam itself was then used to align the optic every ~30 degrees. To perform the alignment, the optic was rotated in the horizontal plane to determine the position of maximum X-ray intensity passing through the pinholes at the front and back ends of the optic. In this way, residual wobble from the mechanical alignment of the optic was removed.

It is important to emphasize that a Wolter-I optic is an imaging instrument. In this way, misalignment of the optic will not cause a displacement in the resulting image. The only consequence of any optic misalignment is that the measurements will be effectively performed at slight off-axis angles that vary as a function of azimuth position. The optic angular resolution is constant up to several arcminutes off-axis and only the throughput will be slightly degraded if the optic is slightly misaligned. Thus, small optic misalignments, estimated to be less than 15”, will not effect the HPD measurements.

To perform the scattering measurements, the optic is translated into the X-ray beam, and the analyzer crystal is rotated to probe the angle of the scattered radiation. In this way, the conic approximation error inherent in the optic design is not measured. The analyzer crystal accepts 5” as a nearly perfect step function. By

scanning the analyzer crystal, a histogram of the reflected X-rays in angle space is recorded. Due to the excellent crystal resolution, essentially no background exists in this measurement and only small systematic uncertainties ( $\sim 5''$ ) are associated with co-adding the individual scans. This metrology method is thus very simple to analyze and provides a very accurate composite two-bounce image of the upper and lower shells at multiple azimuth positions.

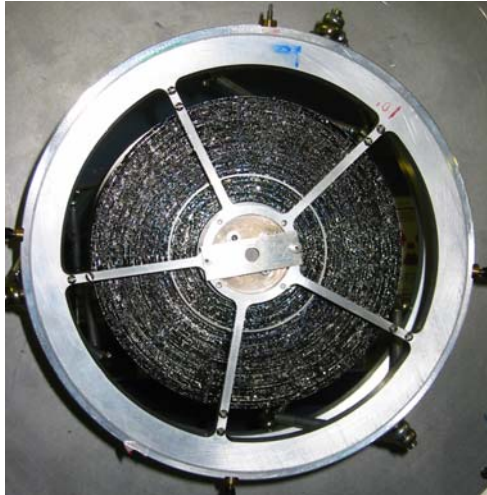


**Figure 2:** End view of the first *HEFT* optic (HF1) in 8 keV X-ray facility.

The BM05 beamline at the ESRF synchrotron facility was used to perform high energy X-ray measurements on the HF1 optic. A double bounce Si(111) monochromator and beam collimators were used to generate an in-plane divergence of  $1''$  for the X-ray beam. The monochromator has an energy range of 15 to 70 keV. The alignment of the optic was performed similarly to the DNSC setup, and as with the 8 keV measurements, pencil beam scans were performed.

For HF1, a CCD detector was used at ESRF to generate a spatial image instead of using an analyzer crystal to measure the angular distribution of the focused X-rays. Due to space constraints, the CCD detector could not be placed at the focal point of the optic located 6000 mm from the optic center, but instead was positioned 2457 mm from the optic center. The only consequence of the shorter effective focal distance is an increase in the conic-approximation error folded into the image. However, this error is still never more than  $\sim 20''$ , and a small correction ( $\sim 3''$ ) is applied to correct for its impact upon the performance of these shells.

Unlike the scanning technique of the 8 keV measurements, a significant amount of background is measured using this imaging technique. While this background is normally quite flat, it does begin to have structure once the total measurement throughput becomes low. However, a background subtraction

procedure has been developed to deal with this problem and is discussed in more detail elsewhere (Koglin et al. 2004a). The systematic uncertainty in these high-energy X-ray measurements is estimated to be  $\sim 10\%$ .

In a later measurement of a prototype optic for *NuSTAR*, we performed high energy measurements at ESRF using the technique of scanning with an analyzer crystal that was described for the 8 keV measurements at DNSC (Koglin et al. 2004b). While this provides for a more precise measurement of the angular resolution (i.e., zero background), it is also significantly more time consuming ( $\sim 15\times$ ) than direct imaging with a CCD. Due to the limited availability of beamtime at ESRF, it is not a practical method for calibrating large optics at multiple energies.

Both 8 keV and high energy (18-68 keV) X-ray calibration data have been previously reported for HF1 in addition to LVDT metrology. The images obtained from these methods are plotted in Figure 3.

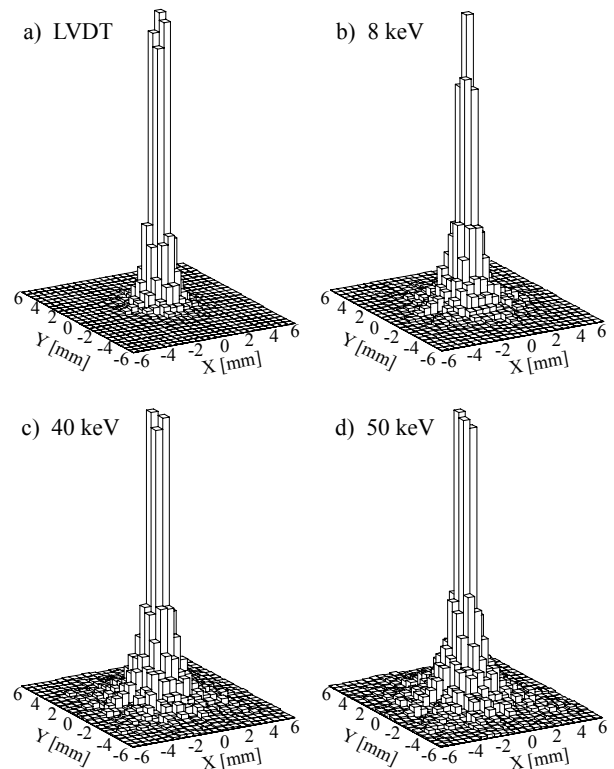


**Figure 3:** An image generated using a ray-trace code with LVDT surface metrology data is plotted in a). Composite images generated from 8, 40, and 50 keV pencil beam scans are plotted in b), c) and d), respectively.

Each independent measurement yielded consistent results, and the HPD performance of the complete optic was determined to be  $1.3 \pm 0.1'$  at 40 keV (Koglin et al. 2004a). A clear improvement in performance was measured after changing from three to five spacers per quint section. The pre-mounted, free-standing

mirrors are only nominally cylindrical with small radial mismatches and twists. The improvement in performance with greater spacer density results from the greater ability to remove out-of-phase roundness errors in the mirrors (i.e., twists such that the nominal graze angle in the mirror changes with azimuth angle). The goal of the mounting method is not to improve the axial figure of the mirrors – the goal is to simply constrain the mirror to the correct radius and angle at the point of the graphite spacers. Away from the spacers, the intrinsic roundness errors in the mirrors will cause the nominal graze angle of the mirror to deviate slightly from the required graze. By increasing the spacer density, this type of error can be minimized. The HF2 and HF3 optics have also been calibrated with LVDT and 8 keV measurements using the same procedures, the results of which have been previously reported (Koglin et al. 2004b).

We have previously conducted a ultra-violet (UV) full illumination test of a prototype optic at the University of Colorado's Center for Astrophysics and Space Astronomy (CASA) using their 'long-beam' vacuum tank illustrated in Figure 4. The UV source originates through a 100  $\mu\text{m}$  diameter pin-hole. The source UV radiation is then reflected onto a parabolic mirror at one end of the tank by a collimating mirror. The parabolic mirror floods the vacuum tank with UV radiation directed parallel ( $<10''$ ) along optical axis of the tank. Since the 6 m focal length of the test optic was longer than the usable length of the vacuum tank, the optic was positioned 3 m from the end opposite the parabolic mirror, and a gold folding mirror was used to reflect the UV radiation focused by the optic back onto a micro-channel plate (MCP) detector. The MCP detector, which was built by Siegmund Scientific, has a sensitive area of 255  $\text{mm}^2$  with 85  $\mu\text{m}$  resolution and operates with a quantum efficiency of about 5%. A sheet of Teflon with an opening for the optic was positioned in front of the optic and MCP to shield the MCP from background UV radiation.

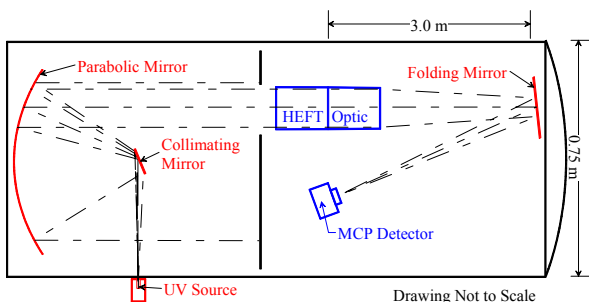


**Figure 4:** Illustration of UV test setup at CASA.

While this method provides no detailed information on the individual optic components, it unambiguously provides a 'what you see is what you get' result for the image requiring essentially no intermediate data

analysis steps. Once the time consuming task of setting up the test hardware was completed, we were able to quickly perform both off-axis and depth of focus studies to gain a more complete understanding of the optic performance. These measurements were consistent with the expected optic response, and the results agreed well with both LVDT and 8 keV X-ray. The good agreement between the X-ray and UV measurements indicate that no difficulties exist in properly aligning the optic for the X-ray pencil beam scans. A more detailed discussion of this measurement is given by Koglin et al. (2003).

#### 4. EFFECTIVE AREA

A highly nested optic is required to achieve large effective area, part of which will inevitably be obscured by structural support. Past soft X-ray telescopes using segmented focusing optics have reported significant losses stemming from geometric factors such as shadowing due to mirror misalignments, but these losses have not always been completely understood – e.g., SODART (Christensen et al. 1997), ASCA (Tusaka et al. 1995), Astro-E (Shibata et al. 2001). In the case of *HEFT* and other similar hard X-ray optics, shadowing becomes especially important due to the smaller graze angles required for hard X-rays. The *HEFT* assembly approach is particularly adept at minimizing such shadowing because each mirror segment is constrained by several spacers machined to the correct radius. However, there will typically be an in-phase roundness error associated with these mirrors as they become slightly displaced between spacers due to radial mismatch (the shells are nominally cylindrical but mounted to a conic geometry), which will cause some shadowing. Losses from shadowing in this manner will be considered to be loss in axial throughput – in contrast to losses from structural obscuration that will be dealt with later.

In addition to assessing the angular performance, the LVDT data was used to determine the axial throughput using raytrace calculations. The result of these throughput calculations are shown in Figure 5. We have also determined the axial throughput at DNSC using 8 keV scattering measurements in a double-axis diffractometer configuration without the analyzer crystal in place. For these measurements, the 8 keV X-ray flux was measured every 2.5 degrees with a pin diode detector and calibrated with the direct beam similarly to the performance measurements. The axial throughput results extracted from this 8 keV data are also plotted in Figure 5 along with an analytic approximation to the 8 keV and LVDT.

For the first 22 inner mandrel layers where only three spacers were used for each mirror segment, the axial

throughput becomes increasingly degraded as the conic angle decreases toward the innermost layer. This trend is expected because a given roundness error will cause a relatively longer shadow for shallower graze angles than the same error will cause for larger graze angles. After the switch to five spacers starting at layer 25, the axial throughput was consistently  $\sim 90\%$ . Because of the good agreement between the LVDT simulation and the 8 keV X-ray illumination measurements, we can be confident that the loss in axial throughput is completely accounted for by geometric shadowing effects. Any degradation in throughput due to other factors such as scattering from dust particles or imperfections in the multilayer coatings must be minimal, as is indeed expected.

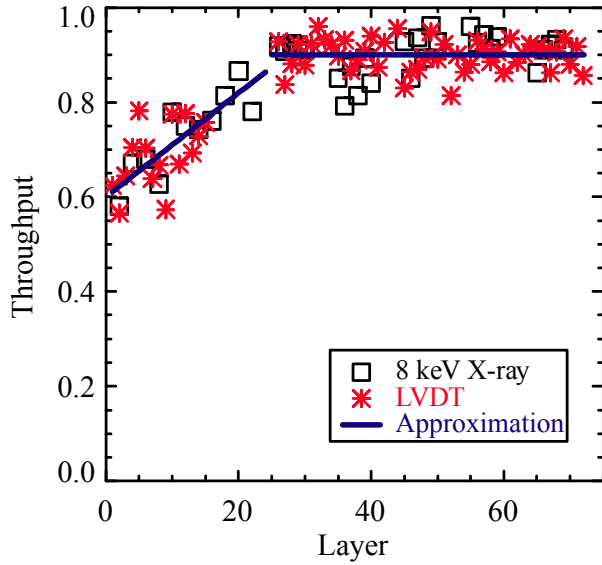


**Figure 5:** HF1 throughput determined from raytrace calculations using LVDT data and measured directly using 8 keV X-rays. The 8 keV measurements are the average for the entire layer as are the LVDT measurements for the inner layers up to layer 16. The rest of the LVDT measurements are typically only for one sample quint segment. The errors in each of these measurements are estimated to  $<5\%$ .

Each *HEFT* optic module was mounted on the gondola using a support structure similar to that shown in Figure 2 that will cover the gaps between quint sections. The five supports will each be  $w_{\text{gap}} = 3$  mm wide – about the same width as the gap between quint sections. While the spacers themselves are only 1.6 mm wide, a small amount of epoxy excess around the spacer will cause added obscuration for each spacer. On average, each spacer obscures  $w_{\text{spacer}} \cong 2.5$  mm of the segment. Thus, the total obscuration will be

$$\epsilon_{\text{obscuration}} = (n_{\text{spacers}} w_{\text{spacer}} - n_{\text{segments}} w_{\text{gap}}) / (2\pi r_{\text{uo}}), \quad (2)$$

where  $n_{\text{spacers}}$  is the number of spacers,  $n_{\text{segments}} = 5$  is the number of mirror segments, and  $r_{\text{uo}}$  is the middle radius of the upper layer. The total obscuration for the first two *HEFT* modules will range from 10-20%.

## 5. HEFT PRE-FLIGHT OPTICS ALIGNMENT

The three flight optics for *HEFT* were co-aligned to focus on their respective CdZnTe detectors using an X-ray source. An alignment fixture was positioned using laser alignment at a distance of  $72 \pm 0.05$  m from the optic entrance. The X-ray source was installed and conditioned in the first optic position. The x-ray generator was operated at a current of 0.30 mA and a voltage of 35 kV. The mean energy of the X-ray source at the optic aperture was approximately 25 keV with a spread of about  $\pm 4$  keV. A aperture on the x-ray tube was adjusted to center the source flux at the entrance of the optic using a NaI detector with crystal diameter of 5.0 cm. The X-ray source produced a flux intensity distribution that was measured to be uniform within better than 20% over a diameter greater than 50 cm (much larger than the optic diameter of 24 cm)

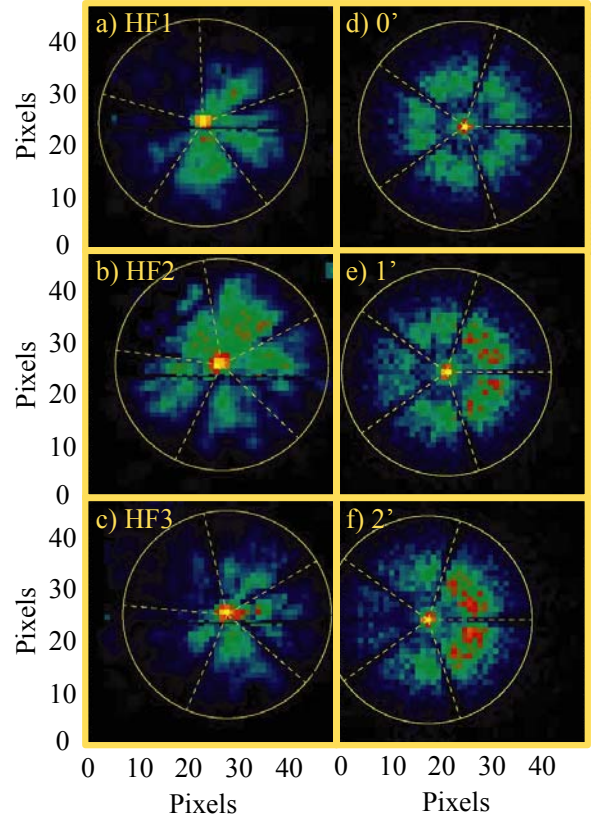


**Figure 6:** Images obtained from a 25 keV source positioned 72 m from the HF1, HF2 and HF3 optics are plotted in a), b) and c), respectively. Simulations for this setup with off-axis sources (i.e., optic misalignments) of  $0^\circ$ ,  $1^\circ$  and  $2^\circ$  are plotted in d), e) and f), respectively. Pixel sizes are  $0.5 \text{ mm} \times 0.5 \text{ mm}$  ( $17'' \times 17''$ ).

A raytrace simulation was performed for 25 keV X-rays to determine the expected image topology for on- and off-axis sources (or alternatively a misalignment of the optic for an on-axis source), in addition to the expected effective area for a source positioned at 72 m instead of infinity. This simulation included

obscuration from spacers and structural obscuration (c.f., Eq. 2), a throughput model based on the measurements shown in Figure 5, and the expected W/Si multilayer response. The simulation also accounts for mirror imperfections using Beckmann scattering theory, with the model parameters (e.g., amplitude and spatial frequency of the errors) adjusted to match the observed response. The simulated images for 0', 1' and 2' off-axis are shown in Figures 5 d, e and f, respectively.

X-ray alignment was performed iteratively by acquiring an X-ray image, comparing it to these simulations and determining how far, and in which direction, the optics needed to be adjusted. This process was repeated for each of the three optics, two of which required adjustments between 1' to 2'. The resulting images for HF1, HF2 and HF3 are shown in Figures 5 a, b and c, respectively. Based on the relative symmetry of these measured images compared to the simulated images, the telescopes appear to all be co-aligned to within at approximately 1'. The effective area was determined from the ratio of the count rate at the detector and the flux density at the optic entrance with a correction factor of  $\alpha=0.687$  for X-ray attenuation over the intervening 6.2 m path, and is given by

$$A_{\text{meas}} = R_{\text{FP}} / (\text{Flux} \times \alpha). \quad (3)$$

The measured data and the theoretical effective area  $A_{\text{theory}}$  are detailed in Table 1. The measured effective area is found to be within 20% of the value expected (with an estimated uncertainty in the measurements of 20% due to source non-uniformity and 10% in the simulations mainly due to uncertainty in approximating X-ray source energy distribution, ~21-29 keV, with a delta function at 25 keV). These effective area measurements, as well as the X-ray images, confirm that the optics were performing as expected.

**Table 1:** Pre-flight effective area measurements

Optic	Flux ph/cm <sup>2</sup> /s	R <sub>FP</sub> ph/s	A <sub>meas</sub> cm <sup>2</sup>	A <sub>theory</sub> cm <sup>2</sup>
HF 1	13.9	189	20	25
HF 2	12.2	190	23	25
HF 3	12.9	160	18	20

## 6. HEFT FLIGHT

*HEFT* was launched from Ft. Sumner, NM on May 18, 2005 at 19:55 UTC. Photographs of the *HEFT* gondola and balloon just minutes before and after launch are shown in Figure 7. The flight was terminated at 20:40 UTC the following day. Observations of Her-X1, Cyg-X1, GRS 1915, 3C454.3, X-Per, and the Crab Nebula were performed over this time. We are currently processing the data and expect to publish results in the near future.



**Figure 7:** Photographs of *HEFT* minutes before and after launch on May 18, 2005 in Ft. Sumner, NM

## 7. NUSTAR

NuSTAR is a small explorer mission currently in an extended Phase A study period. A decision on proceeding to development is expected in early 2006 with a nominal launch date of 2009. The optics design and production process proposed for *NuSTAR* is based on *HEFT* (Koglin et al. 2004b and 2005). The extensive design heritage, calibration techniques and lessons learned from *HEFT* will be employed for *NuSTAR*. For example, smaller mirror segments with more spacers will be used to improve the angular resolution (40'') and throughput for *NuSTAR*.

## ACKNOWLEDGEMENTS

We are very appreciative of the excellent support of the successful *HEFT* balloon flight supplied by the National Scientific Balloon Facility (NSBF). Special thanks to B. Ramsey (MSFC) for facilitating use of an X-ray calibration source and to E. Ziegler and the staff at ESRF for their assistance with the high energy measurements. We are grateful to CASA at the University of Colorado for hosting us as guests at their long-beam UV facility. This work is supported by a NASA grant to Columbia University and California Institute of Technology.

## REFERENCES

- Christensen et al. 1997, Proc SPIE 3113, 294.
- Jensen et al. 2003, Proc. SPIE 4851, 724-733.
- Koglin et al. 2003, Proc. SPIE 4851, 607-618.
- Koglin et al. 2004a, Proc. SPIE 5168, 100-111.
- Koglin et al. 2004b, Proc. SPIE 5488, 856-867.
- Koglin et al. 2005, Proc. SPIE 5900-33.
- Madsen et al. 2004, Proc. SPIE 5168, 41-52.
- Shibata et al. 2001, Ap. Opt. 40, 3762.
- Tsusaka et al. 1995, Ap. Opt. 34, 4848.